CRANFIELD UNIVERSITY

Aimal Mazidi

Feasibility Study of Composite and Multi-Modality Detector Materials Surface Functionalisation Requirements

School of Aerospace, Transport and Manufacturing
Precision Engineering

MRes in Manufacturing
Academic Year: 2016 - 2017

Supervisor: Dr Gregory Bizarri
September 22, 2018

CRANFIELD UNIVERSITY

School of Aerospace, Transport and Manufacturing
Precision Engineering

MRes in Manufacturing
Academic Year 2016 - 2017

Aimal Mazidi

Feasibility Study of Composite and Multi-Modality Detector Materials Surface Functionalisation Requirements

Supervisor: Dr Gregory Bizarri
September 22, 2018

This thesis is submitted in partial fulfilment of the requirements for the degree of MRes in Manufacturing

TABLE OF CONTENTS

LIST OF FIGURES

LIST OF TABLES

LIST OF ABBREVIATIONS

ZnO	Zinc Oxide
LSO	Lutetium Oxyorthosciilicate
LYSO	Lu1.8Y.2SiO5:Ce Cerium doped Lutetium based scintillation crystal
(Ce)	Caesium dopant
PET	Positron Emission Tomography
ToF	Time of Flight
MRI	Magnetic resonance imaging
CT	Computed tomography
BaF2	Barium fluoride
KeV	Kilo electron Volts
WLS	Wave length shifter
LXe	Liquid Xenon
PMT	Photo multiplier tube

Abstract

Reaching social limits within health care, security and energy physics, a demand for development of current technologies in radiation detection is becoming more urgent. A proposition is to develop a multi-modality heterostructure radiation detectors with ability to bypass performance of the current technological limitations. With successful results in this multi-disciplinary research project involving, material processing, computer simulation and manufacturing we impact greatly the social challenges we are facing today such as need for better health care system, safer social security, cleaner and more efficient energy as well as enhancing modern physics.

Global aim of the project is to demonstrate heterostructure radiation detector to have high performance, being ultra-fast, with high stopping power with comparison to the current time of flight positron emission tomography detectors. My part within the project is to improve light transport within the heterostructure by functionalisation all the heterostructure surfaces (Lu2SiO5/ZnO interfaces and outer surfaces).

1 Introduction

1.1 General

This project is part of a larger effort, addressing the current and intrinsic limitations of detector materials by developing a novel family of highly modular heterostructure scintillator. Of interest is the development of heterostructure radiation detector materials as a high performance, ultra-fast with high stopping power, alternative to the current Time of Flight Positron Emission Tomography (ToF-PET) detectors. This is achieved by merging of two scintillators each having its individual advantages; Lu2SiO5:Ce3+ (stopping power), and ZnO (sub-nanosecond time response). Further details about the importance of these two scintillators would be covered in this report.

Scintillators pay a major role in medical imaging and there are many issues in the current imaging modalities as stated in Table 2.1. Amount of radiation dosage the patient receives brings limitations to the imaging resolution for current scintillators available, this is an important factor in medical imaging which is one of the main drivers for the emerging of a new scintillator type.

Research into new scintillators in the recent years has been increasingly successful with growing demand in medical imaging, security and high energy physics leading to development of gamma and neutron detectors and potentially reaching limits in single crystal type scintillators demanding for a new generation of scintillators such as composite/heterostructure type radiation detectors.

Scintillators are materials used for radiation detection and a material that emits light after it interacts with radiation is known as scintillation. Scintillators group with highest amount of luminosities and shortest decay time are semiconductors and therefore, it is very important to study these semi-conductors in plain or composite form. ZnO has a very high density which is useful for Neutron and Alpha radiation. Scintillator materials absorb and convert high energy particles coming from the radiation source into low energy photons (light) [2]. Fast timing emission response, stopping power and light output qualities are desirable for an ideal type of scintillator.

Application	Main Issues
X-Ray	Radiation, Cost
CT	Radiation
PET	Quality
Ultrasound	Cost
MRI	Image Resolution, Cost

Table 1-1: Medical Imaging Modalities

1.2 Scope

This project focuses on designing and optimising the heterostructure layout in terms of light transport looking at Lu2SiO5:(Ce3+)/ZnO surfaces and interfaces. This encompasses simulation of gamma response, simulation of light transport mechanisms. Gamma response, light transport mechanisms, light path, its fate and energy simulated via Geant4 tool-kit.

Simulation to be conducted on individual layouts to compare timing and energy absorption on different layouts. A theoretical suggestion on which deposition method can be used to develop coating is also studied.

2 Medical Imaging - PET

2.1 General

One of the most modern technologies for medical imaging is positron emission tomography (PET) which involves three-dimensional distribution of a radioactive traced element in the human body through injecting the patient. PET enables us to see functional mapping of the cells by function of normal metabolic process of living cell through the interactions of the radioactive tracer which is injected within the body as it spreads to the cells.

Positron Emission Tomography process involves annihilation of electrons which causes emission of two collinear gamma quanta. Opposing detectors in a detector ring is connected within through the coincidence electronics and projections of electronic collimation at different angles are converted to image of the patient using back projection or reconstruction algorithms. Figure 3.1 shows PET process as an illustration.

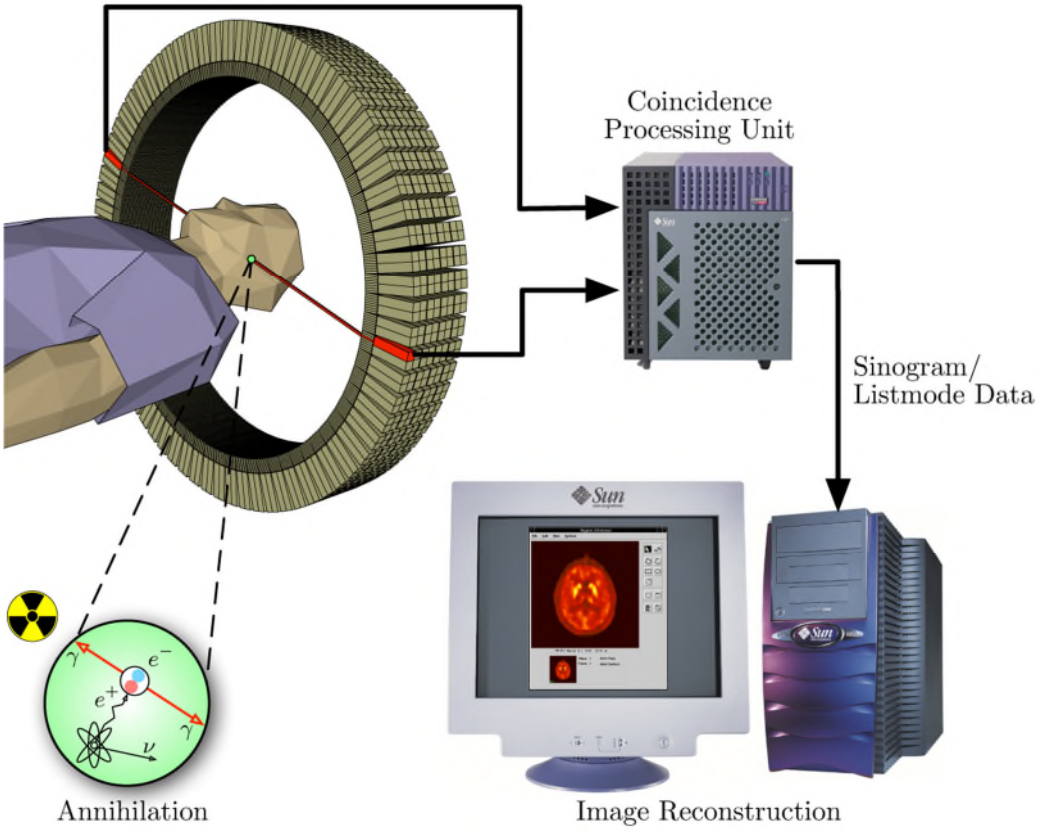

[32]

Figure 2-1: Positron Emission Tomography procedure

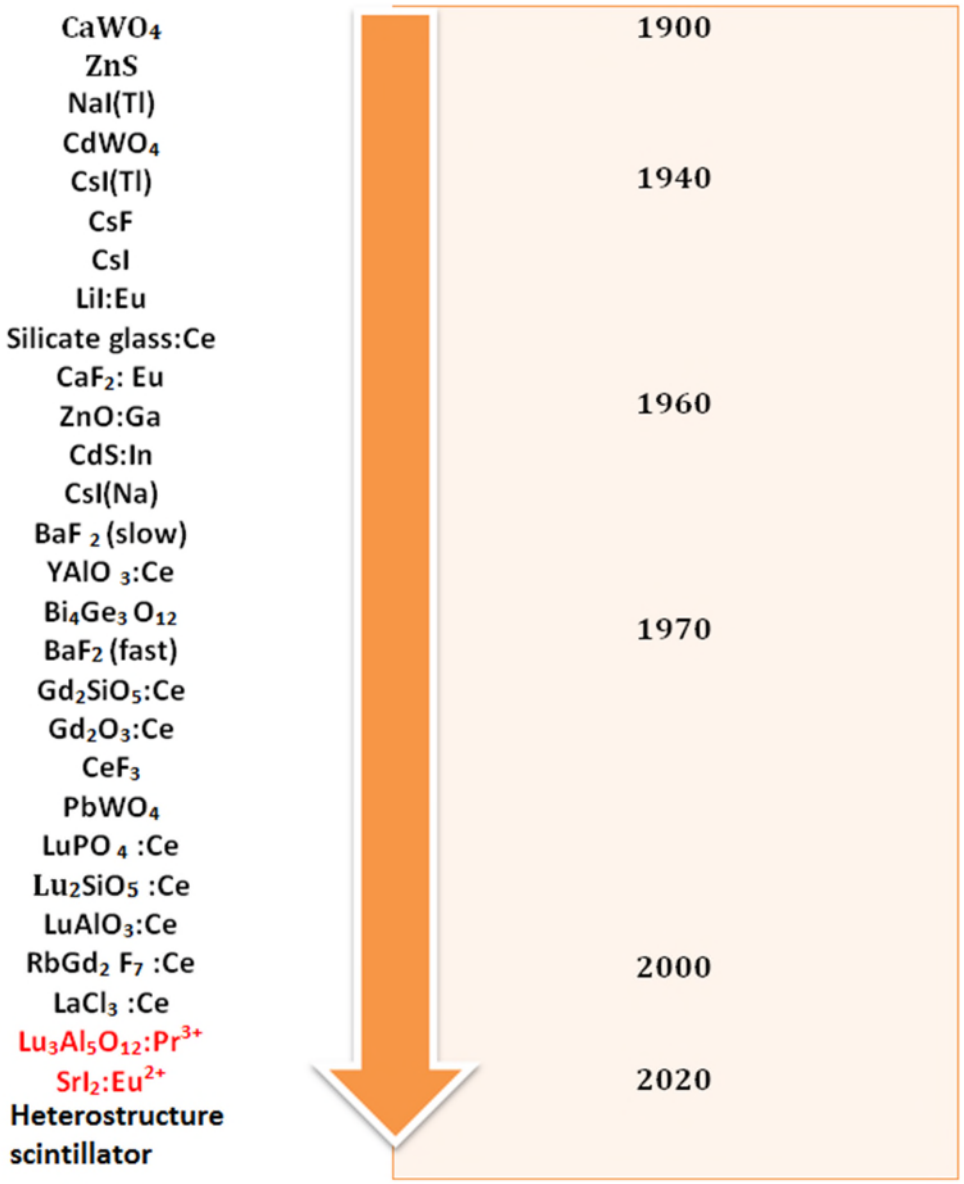

Figure 2-2: Quest for an ideal inorganic scintillator

2.2 The quest for an ideal scintillator

In the past century several types of inorganic scintillators have been developed such as the list provided in Figure 3.2. The first inorganic scintillator used in a device was ZnS in 1903 for screening and scintillation produced was visible to the naked eye under a microscope in a dark room. ZnS has a very low light yield to meet the requirements for PET. A new technique to measure the scintillation was developed in the 1940s and scintillators like CsI are still being used since then with such development. CsI has very good light yield however the decay time is very poor for PET application. Some of the discoveries such as BaF2 which have been vastly used within high energy physics and medical imaging drawn by research into development of scintillators for precision calorimetry and many other scientific and industrial applications. Newly developed inorganic crystals include lanthanum chloride doped with cerium as well as cerium doped lanthanum bromide. This new development is a very important stage in scintillators discoveries as it has been able to provide excellent properties, however these have been a compromise in either decay time or light yield instead of a combination of high performance of both properties.

This brings the need for a new type of scintillator, composite combination of ZnO and LSO.

2.3 Applications

Sodium iodide doped with thallium has a very high light yield [19] and has been used widely in gamma radiation detectors in the recent year due to its relatively good scintillation properties. However very large crystals are required which is not only very expensive but also very hard to manufacture. Lutetium Oxyorthosilicate (LSO) scintillators like LYSO and LFS all are single crystals doped with lanthanide elements to achieve desirable scintillation properties. Lanthanide based scintillators have been used widely among modern medical imaging technologies for their excellent stopping power abilities for gamma rays as well as very high light output properties. However due to relatively long decay time of 40ns compared to some scintillators, such as ZnO with sub nanometre decay timing, it is a compensate for the current technology and waiting for new technology to develop and fill the gap. ZnO on the other hand is not suitable as a single crystal scintillator as stopping power and light output properties are not as good as of LSO and it may not be practical, in terms of size, to grow a single crystal ZnO to achieve desired stopping power and light output properties.

2.4 Performance characteristics of PET scanners

2.4.1 Technology and Physics

Ionizing radiation is radiation that carries enough energy to liberate electrons from atoms or molecules, thereby ionizing them. All types of ionizing radiation particles: Alpha particles, Beta particles or Gamma rays happen due to unstable atoms, Figure 3.3. These atoms either have extra energy or mass or even both. To reach a stable state these atoms must release this extra energy or mass or both mass and energy in form of radiation. Two types of radiation can occur. Direct radiation which interacts with other atoms directly if the charged particle has enough kinetic energy. Direct ionizing radiations are massive charged particles such as Alpha, Beta and neutron particles. Indirect ionizing radiation on the other hand does not interact with matter strongly as it is electrically neutral but can ionize atoms indirectly through Photoelectric and Compton effect. Gamma rays and x-rays are indirect ionizing radiations.

Electromagnetic radiation unlike alpha and beta radiation does not consist of any particles instead it consists of a photon of energy which is emitted from an unstable nucleus.

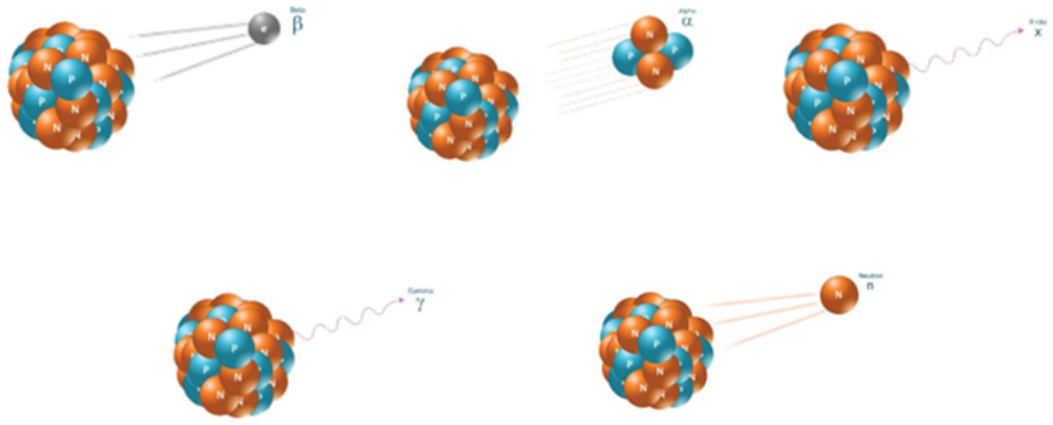

[33]

Figure 2-3: Alpha particle, beta particle, neutron particle, x-ray and gamma ray radiating from an atom

2.4.2 Converting ionizing radiation into usable signal

Material doping is introduced to semiconductors such as ZnO to improve some of the material properties by adding impurities to the lattice. Typical doping elements are; boron, arsenic, phosphorus, and gallium which create an electron hole in the lattice, electrical conductivity is improved as a result. Some elements when used to dope ZnO can create donor levels in the lattice and co-dopant elements can create forms of shallow acceptor levels. Research has been studied on combination of the two types, donor and acceptor levels which show that acceptor level types strengthens the intra-band luminescence but weakens the edge luminescence. By controlling the concentration of the dopant and co-dopant it is possible to change the intensity of the edge band and the intra-band luminescence of ZnO.

Scintillation process can be described in three sections. An ionizing radiation in our case gamma-ray is absorbed by a scintillation medium for example at our inorganic ZnO material. In simplistic form we can described this process as following, the high energy is absorbed and converted into low energy photons. Low energy photons converted into electrical signal using a detector. There are many different types of detectors available to use depending on the type of radiation being detected and scintillation medium used. Some of the detector types commonly used in recent years are: photomultiplier, avalanche photo-diode, silicon PM, solid state or vacuum detectors.

Scintillation mechanisms depend on the energy state of the material in the crystal lattice and in doped crystals they also depend on the activator as well as the energy state. The width of the band gaps depends on interactions between the atoms and the ions in the lattice. Conduction band, valance band and forbidden bands exist. Electrons in the conduction band can mitigate throughout the crystal. In the valance band the electrons can absorb energy by interaction with photo electron or through Compton scattering. Doping is usually introduced to the crystal to shift the emission wavelength from ultraviolet to visible range because when the electrons return to ground state and emit scintillation photons the photons have so much energy that the emission is in the ultraviolet region. Within

the forbidden band gap energy states are created to allow electrons to de-excite and go back to valance band.

2.4.3 Matter interaction

A scintillator material configuration consists of several states such as core level, valence band, and conduction band. Radiation interaction occurs between the valance and conduction band. As the ionizing radiation is absorbed at the conduction band, the radiation energy carries through the lattice looking for a more suitable configuration and then as it finds the dopant ions we have a photon emission. This is illustrated, in Figure 3.4, in form of three stages. We will consider these three-electromagnetic radiations interact which would occur at our scintillator if a gamma ray is emitted upon it:

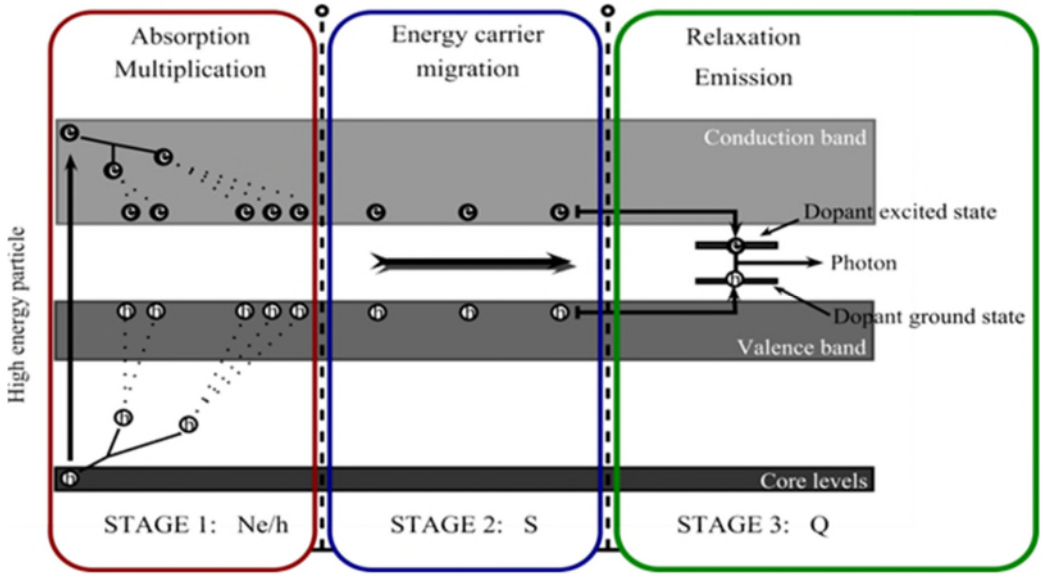

[34]

Figure 2-4: Matter interaction, scintillation to relaxation

2.4.3.1 Compton effect

Compton effect process involves an elastic collision between the photon and the electron, resulting in creation of scattered Compton electrons and Compton photons. Number of charge carriers produced in the scintillator medium is affected during Compton scattering that is if the Compton scattered photon leaves the scintillator medium but then is reabsorbed back in the scintillator through the

photoelectric affect thus the number of charge carriers produced in the scintillator is the same as in a single photoelectric interaction. The diagram in Figure 3.5 shows incident photon of energy hv interacting with an electron at rest. The scattered photon with energy hv' scatters at an angle relative to the original momentum vector. Mass energy of an electron at a rest state is 511keV and when collision occurs the Compton photon and Compton electron created would have less energy as they are scattered.

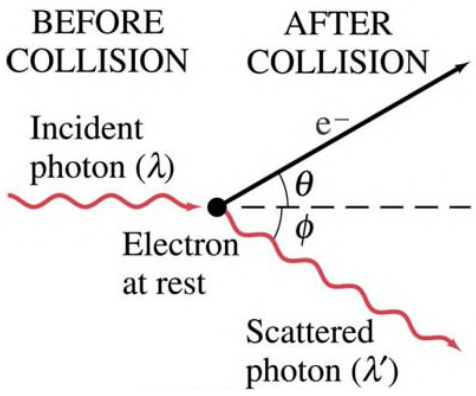

[35]

Figure 2-5: Incident photon of energy hv interacting with an electron at rest

2.4.3.2 Photoelectric effect

This is the most dominant process where the inner shell can absorb the photon energy completely and therefore the electron has enough energy to leave the atom. The hole created would within the nucleus would be ionized as the electron coming from higher energy level would want to fill it. As this process occurs X-rays are emitted because of radioactive transition. However, if the transition is non-radioactive auger electrons would be created instead on x-ray emittance. This process is illustrated in figure 3.6. The probability of photoelectric emission is strongly influenced by the energy of the incident photon which coincides with the ionizing energy of the specific atomic electron shell.

2.4.3.3 Pair production

Pair production is creation of particle and antiparticle element and is the dominant matter interaction process under high energy phenomena with required energy

of 1.022MeV to start, which is a total mass energy of 2 particles. Moreover, pair production takes place in the coulomb field of a nucleus and not the atomic electrons. Electron-positron pair is produced with this type of interaction from a photon particle. However, to satisfy the conversion momentum from photon to electron.

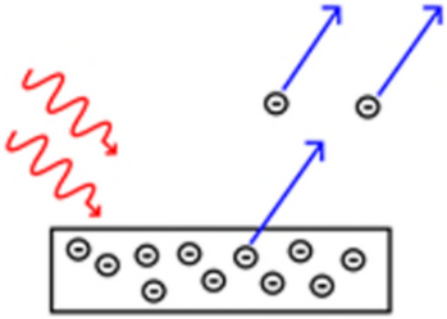

[36]

Figure 2-6: Photoelectric Interaction Probability positron pair the photon must be near atomic nucleus as the energy and momentum conversion in free space is not possible.

Bremsstrahlung radiation is produced when electrons are ejected from parent atom during deceleration of particles in medium. This is also called hard collisions as the charged particles interact energetically with the nucleus. Once the electron is ejected from whichever shell; M-L-K, there will be an empty state or a hole in that shell. The electrons from the higher energy states will want to fill this empty state. The energy required to fill the hole is less than that of the electron coming in from the higher energy shell and therefore an excess energy is emitted as form of x-ray of gamma ray. [1] A photon of energy will also be emitted during this bremsstrahlung production where the energy of the photon is equal to the binding energy between the shell levels from where the electron has originated to the where the empty state is as shown in illustration on Figure 3.7.

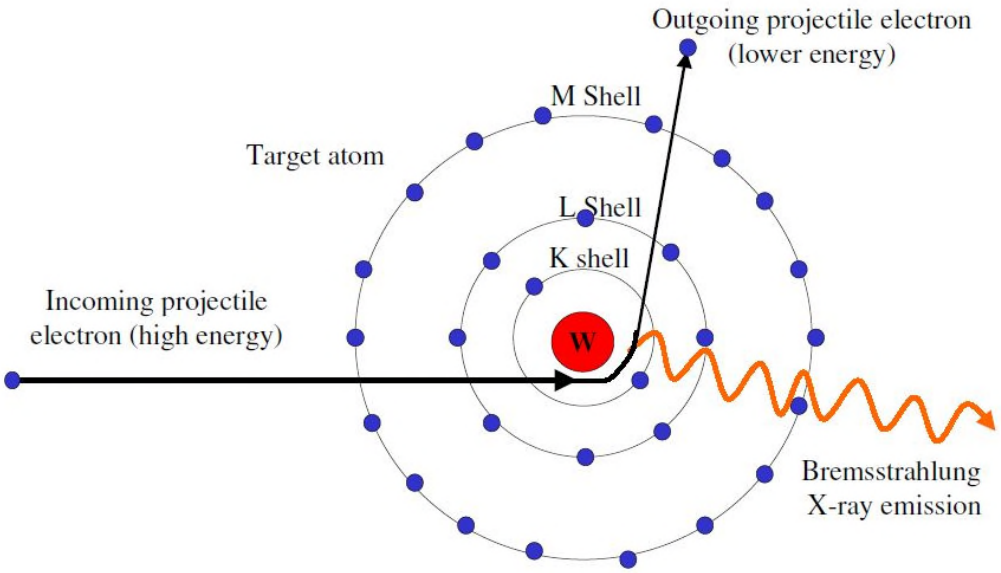

[37]

Figure 2-7: Bremsstrahlung production

2.5 Conclusion

Many of the current successful PET systems use a light sharing detector with pixelated lutetium-based scintillators and a large photomultiplier. One of the main parameters determining the timing resolution is the scintillator thickness. Intrinsic performance limitation of the scintillators is highly dependent on lanthanide doped materials but is unavoidable due to its desirable light output, stopping power and energy resolutions.

Applications in medical images such as in ToF-PET has these basic standard need: high stopping power which means need for high density and high Z element, sub-nanosecond response time and a high light output meaning need for a good energy conversion efficiency. Current scintillators such as LSO and LYSO are only a compromise of the application needs as it lack in timing response of sub-nanosecond requirements. As the latter of current scintillators are intrinsic to lanthanide doped materials there isn't an easy answer to the application needs as removing the dopant from the latter would cause light output degradation and keeping it would not allow for sub-nanosecond response timings. Similarly, for other fields such as security applications, gamma detection is only possible with density materials with high Z elements whereas neutron detection imposes scintillator to be of light elements.

Non-proportionality in the light yield is known to be the major limitation of the energy resolution. Furthermore, studies of correlation of the intrinsic energy resolution of some crystals such as LSO and LYSO show that the intensity of the afterglow of the crystal affects the energy resolution of the scintillation detection [25]. Although afterglow of the crystal can affect the energy resolution there are other factors which can also contribute to it.

LSO and ZnO materials are the bases of this projects aims and objectives as the use of these two materials in the detector will give desirable stopping power and response time due to the intrinsic performance characteristics of the crystals.

3 Multi-functional composite materials concept

3.1 General

Heterostructure detector concept is extended to multiple materials and composites of single crystals, thin films, inorganic, organic and more. With this approach we can utilize multiple materials to meet tight application needs. Using a successful medical imaging scintillator such as LSO crystal the aim would be to design a scintillator around the LSO matrix with intention to maintain the stopping power and light output qualities. An additional scintillator material would be embedded into the matrix allowing for ultra-fast signal response. ZnO material is one of the most fastest known scintillators which would potentially be the ideal scintillator for this purpose and determining the correct composite and design of this heterostructure material is the focus of this global project through materials, manufacturing, simulation and optimization techniques.

Having successfully developed the heterostructure detector would be increasingly beneficial for socially. Patients injected dose would decrease, improving diagnostics, and increasing treatment accessibility and cost. Similarly, success within such design would create many research opportunities in the optimization of different material and manufacturing techniques which could be implemented.

3.2 Material characterization

3.2.1 Structural

To meet application needs we first need to understand what parameters of material influences the performance and why. The stopping ability of the scintillator can be maximized with increase in density and atomic number. Similarly, we can control the amount of scintillation material used to depend on how dense the material is. Chemical stability and mechanical strength are considered during development stage of a scintillating material, some of these are; environmental and chemical durability, ruggedness and mechanical shock resistant, light output with time and temperature variations and sensitivity to moist, air or light [24].

Zinc oxide has a very short de-excitation time of 0.7ns when doped with gallium as well as having a very luminous yield of 15,000 photon/Me V Zinc oxide possesses large fraction of ionic bonding and has a hexagonal wurzite structure with a=3.2497 and c=5.2069 crystal structure giving c/a ratio value of 1.602 which is not very far from ideal value of 1.63. Zinc oxide has a refractive index of 0.009 at 405nm and oscillates from 0.016-0.018 at visible region. ZnO has relatively small band gap of 3.37eV and therefore their conversion efficiency is relatively high [17].

3.2.2 Refractive index mismatch

This is an optical property which is the main factor of this project. With a composite and multi-modality detector material we aim add coating layers of the detector material to minimize the refractive index mismatch between the composites and maximize photon collection. Currently refractive index of most scintillators is, n=1.8-2.2 and n=1.4142 for solid scintillators. with critical angle less than 45 degrees. It may be impossible to solve this completely but matching refractive index would reduce effect of losses greatly. Refractive index is further analysed in the next chapter.

3.2.3 Performance

Luminescence of a scintillator depends on several factors such as; emission wave-length: will determine what detector type to use, light yield: is critical for particles with small energy to improve accuracy and resolution, radiation hardness: considers radiation damage which is important when dealing in high energy physics, proportionality between average energy needed to create an electron-hole pair and recoil electron energy: can cause degradation in energy resolution and decay time: this determines the timing resolution and is a very useful factor to consider in medical imaging.

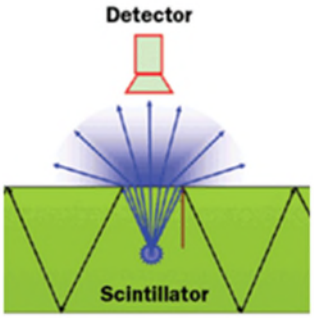

[24]

Figure 3-1: Refractive index (directional change of photonic beam)

Depth of interaction is very important as it is what determines the detection of the scintillation light from the radiation. Using this information, we can measure the arrival of scintillation photons and therefore determine uncertainties in timing [25].

Scintillators with Pr3+ activated dopant have shown possible decay times of twice as fast. I.e. in LuAlO3:Pr3+ decay time of 9ns is observed. And Ce doped scintillators have also shown improvement to scintillators to reach the fundamental limits of around 15-17ns in LaCl3 and LaBr3. However, Eu doped scintillators has not shown very good improvement in decay time. [13]. There are intrinsic scintillation properties with single crystal scintillators such as (brightness, rise and decay times) Lu2SiO5:Ce has high density (7.4 g/cc), effective Z of 66(effective atomic number), an emission spectrum at room temperature is peaked around 420 nm. An article [5] studied energy resolution of LSO: Ce and conducted an experiment with XP5500B PMT detector and at 662keV gamma

ray source, experimental k ik kikons yield = 9,990+-500phe/MeV, Light yield= 30,300+-3000ph/MeV with Energy resolution of 8.3percent+-0.3. Fast decay constant (30percent) = 12ns, slow decay constant (70percent) = 42ns [10, 8, 7].

ZnO: Ga has a very fast decay time of 0.7ns, density of 5.61g/cc, light output of 15,000 ph/MeV, effective Z of 64(effective atomic number), with peak in emission spectrum at 378nm [9]

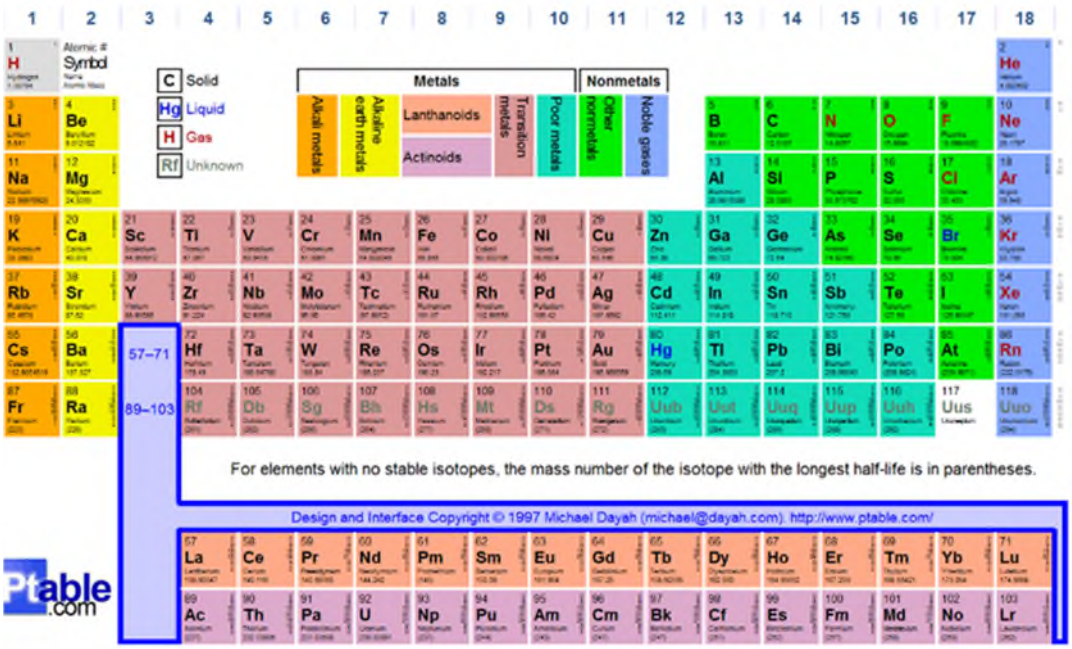

[38]

Figure 3-2: Lanthanide elements within periodic table

3.3 Configuration of the detectors

When gamma ray incidence hits a medium scintillator, due to matter interactions photons are emitted. Every photon that is emitted has a wave-length/energy. To minimize the response time, we would like for as many photons created to be emitted into the PMT (photomultiplier tube) to be detected. This means if we have 10percent of gamma rays deposited onto ZnO we would expect to have photons emitted with the full 10percent of the absorptions. Moreover, we would also like to have all the emitted photons to be detected at the PMT, however some photons may leak out of the ZnO which will reduce the response time. To minimise photon loses at surfaces of the ZnO a reflective layer will be implemented. Light loses due to refractive index mismatch at the detector surface can be minimized by adding an optical coupling between the heterostructure and the detector. An analyse, and review into improvement of the light transportation from photon creation to time of detection is composed.

3.4 Surface functionalisation

3.4.1 Surfaces

To maintain the light impinging on the PMT a special coating is required between the heterostructure scintillator and the detector this coating material allows optimal light distribution and to guide the light towards the detector [17]. Reflective surface coatings act as light guides which increases scintillator efficiency as the number of the photons reaching the detector is increased. An article [28] show very good light transport on scintillators when coupled with light guides which are appropriately coated with good diffuse coating, resulting in large locus dependant variations of light collection.

Light guide coatings used on scintillators can have different functions depending on the material and manufacturing process used. There are two types of optical reflector coatings commonly used on scintillators, diffuse (Magnesium oxide, barium sulphate, titanium dioxide) and specular usually aluminium or an aluminium alloy. Literature shows benefits with both types of optical coatings dependants on functionality required. Specular reflectors are more beneficial for cylindrical shape scintillators on all surfaces except surface in contact with detector. For exit surface diffuse reflector is recommended to avoid light trapping and enhancing in light output. Similarly, light losses in cylindrical shape scintillators are reduced via specular coatings as the coating acts as a light guide and direct the photons towards the PMT detector. On the other hand, in diffuse coatings photons are scattered in a random direction. Furthermore, when considering light losses due to internal reflections diffuse coatings are found to be more efficient. A further review of both type of these reflecting coating is review as both may be used in our scintillator.

Optical properties of the scintillator are very important in light transportation (absorption and scattering, surface finish, and external reflector) Lu2SiO5:Ce has a refractive index of 1.82 at peak wavelength of 420 nm.

ZnO:Ga has refractive index of 1.73 at peak wavelength of 390 nm. At 390 nm wavelength, absorption coefficient is 21.94m, and reflectance is 0.055.

It is noted that optical properties and desired results of the thin films coatings are not only determined from the material/composition used but also the deposition technique used to form the coating. This shows how manufacturing process for performing such thin film coatings pays vital part on the final results and performance of the thin films.

3.4.2 Interaction of light with surfaces

3.4.2.1 Transmission

Light transmission is highly important within scintillator materials. The design of multi-functional composite detector consists of having cylindrical inserts within the single crystal where a fast scintillator material with decay time of sub nanometres can be introduced. ZnO has decay time of 0.7nm [21] and density of 5.6g/cm3. This fast decay time would make ZnO one of the ideal materials to use in this instance.

3.4.2.2 Absorption

To detect gamma rays the scintillator material requires to absorb gamma photons. For medical imaging PET, photons have initial energy of 511keV and two main interactions would be photoelectric effect and Compton scattering.

3.4.2.3 Reflection

An interesting article [15] studies coating materials on glass substrates for reflective purposes. Optical properties of thin film coatings depend on several factors such as the use of thin film material/composition, the substrate surface quality and deposition technique used. This paper studies the principle of optical properties of thin films in form of their spectral characterization as reflectance, transmittance and absorption for a wavelength in a spectral range. It is mentioned that aluminium has very high reflectivity but is unsuitable for window application due to its high transmittance in the visible range however gold and silver thin films have high transmittance in visible range.

Timing for light collection at the detector is very important in PET application as it acts greatly in contribution for overall timing resolution of scintillators. Articles [11] and [22] presents detailed analysis into light propagation and extraction

modes in LSO crystal. A well-designed photonic thin film enhances the light output of dense scintillators with a high refractive index. Photons that are inside the crystal and impinging at angles greater than the Brewster angle (and thus usually undergo total internal reflection) can be transmitted, thus increasing the amount of scintillation light extracted.

Article [24] considers light output properties of photonic crystals as thin films, coated on scintillators in more details. The article uses Monte-Carlo program to simulate light propagation as well as paying close attention to the light output results. Results of some of the simulations of different lattice types where manufactured via sputtering deposition and coatings quality of the nano lithography analysed using scanning electron microscopy (SEM). Best sample showed light yield improvement of 56 percent compared to unstructured reference. Simulations showed that increasing refractive index of material also increase the light extraction and best results gained from around 2.4 to 2.5 material refractive index. TiO2 and gallium nitride where good candidates. Simulation also showed over 50 percent increase in light extraction of GaN compared to Teflon wrapping or glue coupling.

Multi-layer polymer mirror thin film with thickness of 0.065mm have been used in scintillators such as LYSO single crystal size of 1.46mmx1.46mmx4.5mm from article [15] shown to have 99percent reflectivity.

3.4.2.4 Optical reflectors

One type of optical reflectance is a diffuse reflectance. Diffuse reflectance materials reflect light in a uniform way and an ideal diffuse reflector is a Lambertian surface which has 100 percent reflectance independent of direction. Some diffuse reflectors available with up to 98 percent reflectance at 310 nm to 1700 nm wavelengths. Although a minimal thickness of 4mm is required for such reflectance [18].

An article [16] describes use of both diffuse and specular optical thin film coatings on scintillators, their uses, purpose and manufacturing technique used to implement the coating. Magnesium oxide, a diffuse optical coating has been used

as thin film coatings at the proximal end of the scintillator which is known to greatly increase light collection. Specular coatings applied on scintillators with elongated cell structures have shown an increase in light detection this is because with elongated structure photon follows one direction path which is towards the detector and therefore reaches the detector efficiently.

Specular reflective films coated at the proximal end of the scintillator are sensitive to light trapping, when a photon reaches the exit surface of the scintillator at an angle greater than the critical angle it is internally reflected and when photon approaches the exit surface the second time at the same angle of incidence it will internally reflect again and may repeat this infinity which is termed as light trapping. With diffuse coatings on the other hand, angle of reflection changes as so if the photon had initially gone through internal reflection it will most likely not encounter internal reflection at the exit surface the second time. However, with the diffuse coatings, light losses are more probable than in specular reflective coatings as specular reflective coatings act like light guides and target the photons towards the exit face.

It is recommended [16] that increasing in reflectivity of coating does not de-trap a ray which has been through total internal reflection, however increasing the reflectivity doesn’t necessarily increase the trapping but only helps to increase probability of rays reaching there at an angle smaller than the critical angle.

Material	Refractive index	Reflectivity	Reflection type
Aluminium	0.541	0.923	Specular
Titanium	2.16	0.62	Diffuse
Platinum	1.78	0.569	Specular
Barium Sulphate	1.637	0.84-0.98	Diffuse
Teflon tape	1.341	0.99	Specular
Tyvek*	1.51	0.97	Diffuse
Gold	1.5029	0.37	Specular
Polytetrafluorethylene	1.35	0.99	Diffuse

Table 3-1: Type of reflection, refractive index and reflectivity at 420 nm wavelengths *high-density polyethylene

3.4.2.5 Functions of refractive index

Refractive index of a material is found to be very important factor when considering thin film coatings regardless of the function of the coating. E.g. To develop a reflective coating, we require a material with high reflectivity but also refractive index of coating material will need to match that of the refractive index of the scintillator as mismatch in refractive index showed decrease in the efficiency of light extraction due to light trapping problems. Similarly, refractive index is also important when developing a photonic coating for maximum light extraction. Mismatch in refractive index at the proximal end of the scintillator, light can bend and therefore either internally reflect or lose its energy before extraction. However, in this case high refractive index coatings are ideal to increase light extraction and direct light towards the detector by reducing internal reflections.

It is known that internal reflections in specular coatings occur at polished surface for angles of grazing incidence when the refractive index is smaller on the outside surface of the material then the refractive index on the inside surface. Thus, for the thin film coatings which goes in between the LSO and ZnO materials the coating refractive index must match the refractive index of the two.

Article [3] shows how matching the refractive index of the coating with the refractive index of the scintillator pays a great role in the light collection efficiency.

Experiment on four different type of surface quality coatings were accessed where

the scintillator refractive index was 1.66; uncoated polished surface, coating with refractive index of 1.5, coating with refractive index of 1.56 and coating with refractive index of 1.6. Coating with refractive index of 1.6 and uncoated polished surface gave highest percentage of around 90 percent efficiency. Coating thickness did not influence the light collection efficiency where thickness of 0-1-micron coatings where tested. Rough coating decreases light collection efficiency even more than rough un-coated surfaces and best results achieved with polished surface smooth coating with matching refractive index.

3.4.2.6 Other factors in optical coatings

From articles [3] and [24] we can see that there are more factors to consider apart from reflectors, absorbers and diffuser coatings are; surface finish of the crystal, surface treatment and edge effects which found to have great contribution to the light distribution on the face of the crystal.

Surface preparation and coupling methods on scintillators to improve light transport have been studied. Considering 8 different coupling methods (air, three optical gel, an optical curing agent, uv light, cyanoacrylate glue and acetone), optical gel coupling showed best results in terms of light collection using a charge-coupled device CCD camera. Lambertian reflectors (e.g. tephlon tape) and specular reflectors (e.g. ESR enhanced specular reflector) are popular within the scintillation detectors usually coupled with optical grease.

3.5 Light transport

Geant4 tool-kit is used to simulate light transport and decay time of gamma on heterostructure layout. 3D Design is modelled via solid-works software and STL assembly drawings are used within the Geant4 program. Geant4 program is compiled and run to account for probability of event absorption in the heterostructure. The set-up also consists of a detector part which measures the response of the system.

When a photon hits the surface, we can calculate the direction and the attenuation of the reflected ray using Fresnel formulas. When designing a new scintillation detector for nuclear medicine, modelling light transport accurately is essential and previous studies have used Geant4, simulation platform to determine fate of the optical photon. The travel paths also showed how individual photons were affected by different factors such as the reflector and surface finish.

Analysis and comparison of the emission spectrum of the two materials will be used for accounting surface and optical parameters for simulating light transportation as well as validating simulation accuracy. Optical properties such as index of refraction and the reflection coefficient are considered to simulate possible reflection under polished, ground, painted or metallized conditions, considering Snell's law to determine the optical behaviour of the real surfaces. Snell's law states that ratio of sine's angles of incidence and refraction of wave are constant when passing two given media.

To simulate a surface other than a perfectly smooth surface between two mediums we can use Surface-to-surface class. Surface models, surface types and surface finish can be specified. Surface and its properties must be specified together with photon direction of flight which can be specified and defined which help as accurately track photon transportation considering reflection, refraction or transmission at surfaces.

Boundary processes are to be defined when considering optical photon transportation, as a photon arrives a medium boundary its behaviour will depend on the two material properties that joint at the boundary. The photon can either internally reflect, refract, reflect depending on the photons wavelength, angle of incidence and the refractive indices on both sides of the boundary.

To consider for full response of the system, to account for gamma ray absorption, matter interaction, photon creation and photon detection, a design is developed of the simulation set-up. Due to matter interaction photons are created (illustrated with a red X on the Figure 4.3). A reflective surface coating around the cylinder to act as a guide and direct photons towards the PMT entrance window 26in yellow.

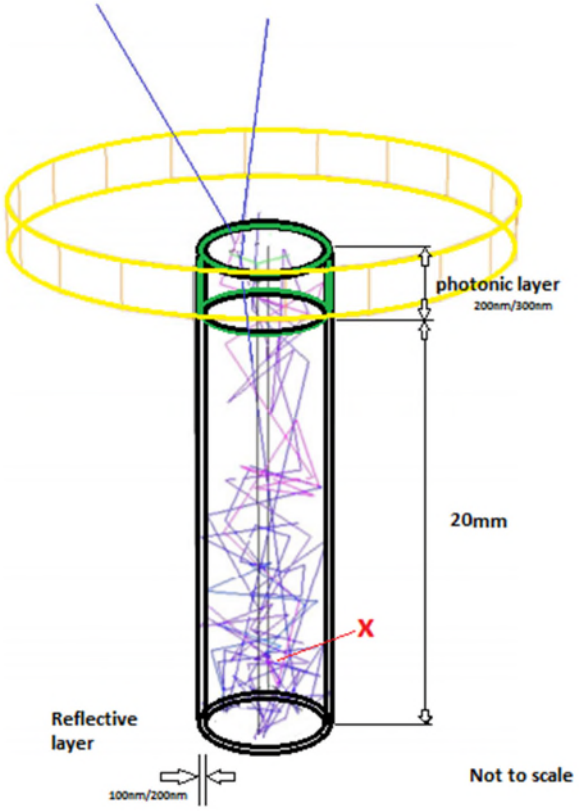

Figure 3-3: Simulation design

Running simulation on selected materials would determine most efficient light transport considering, coating material and coupling used, parameters for the simulation. Developing a summary of input parameters helps when creating design of experiment for simulation as shown in Table 4.2.

Medium	Parameter	Type of variable
Scintillator	Topography	Matrix Vector
	Refractive index	Scalar
	Scintillation emission spectrum	Vector
Coupling	Refractive index	Scalar
	Bulk absorption	Scalar
Reflector	Type (specular of Lambertian)	Name
	Reflectivity spectrum	Vector

Table 3-2: Summary of input parameters for simulation

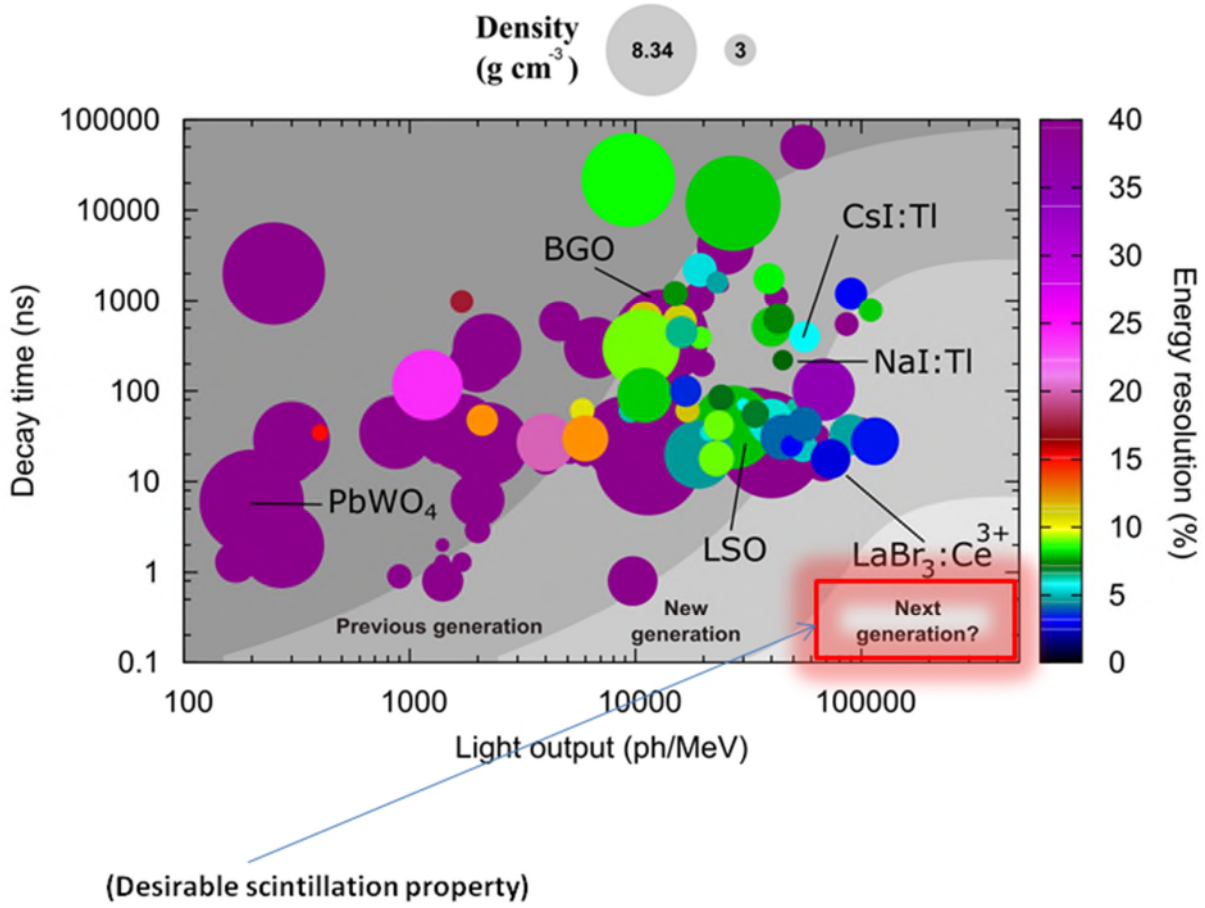

Figure 3-4: Discovered scintillators and future desirable movements

3.6 Time of flight

Response time of scintillators has been reviewed in several articles in aim to increase the signal to noise ratio of an image in PET scanners [2, 12, 4]. Several factors determine light transport and collection at the detector.

3.6.1 Photon Interactions

Production of an optical photon in a detector is primarily due to the Cerenkov and Scintillation processes. As an optical photon is generated it undergoes three kinds of interactions:

1 Elastic (Rayleigh) scattering: Scattering of light by particles in a medium, 29 without change in wavelength.

2 Absorption: Very important for optical photons as it determines the lower limit

of lambda. Also, absorption competes with photo-ionization in producing the signal in the detector, so it must be treated properly in the tracking of optical photons.

3 Medium boundary interactions. As a photon reaches the boundary of a di-electric medium its behaviour depends on the nature of the materials, which join at boundary.

For dielectric - dielectric photon can be transmitter or reflected for dielectric - metal; photon can be absorbed by the metal or reflected into the dielectric material. Absorbed photon can be detected according to materials photoelectric efficiency. For dielectric - black material; here photon is fully absorbed and not detected 5.4.2

3.6.2 Tracking photon on its path

Optical photons are subjected to the in-flight absorption, Rayleigh scattering and boundary action as stated above. The status of the photon is determined by two vectors; momentum of the photon and its polarization.

Photons produced by Cerenkov effect and scintillations are linearly polarized. Therefore, we consider Reflection and transmission probabilities, which are sensitive states of linear polarization (Figure 4.5).

```
Photon at Boundary!
thePrePV:  PbF2_Crystal
thePostPV: World
Old Momentum Direction: (0.291276,0.24402,0.924993)
Old Polarization:       (0.00363557,0.96663,-0.256149)
New Momentum Direction: (0.291276,-0.24402,0.924993)
New Polarization:       (-0.00363557,0.96663,0.256149)
*** SpikeReflection ***
Photon at Boundary!
thePrePV:  World
thePostPV: PbF2_Crystal
*** StepTooSmall ***
```

Figure 3-5: Event run showing photon reflection at a boundary with direction and momentum

3.7 Conclusion

Heterostructure configuration of the composite scintillator provides the detector with minimal response time due to high percentage of energy absorption within ZnO. Furthermore, for competitive event absorption, configuration with minimal 90% absorption of LSO is required. Understanding the physics of light transportation within the medium and acquiring correct surfaces we can control optical photons generated within the separate mediums and therefore allow optimal use of number of generated photons. There are two obvious techniques to find energy absorption and response time taking into account the physics of light transport;

- Developing a complete detector setup including scintillator, PMT, hosing, source and computer to compute the data.
- Create a simulation setup on Geant4 tool-kit

The second option would be a cheaper and faster way to create a prototype layout of the proposed scintillator.

Establishment of materials for surfaces has a great impact on the overall performance of the scintillator and the simulation results due to the physics of light refraction and reflection.

4 Composite material

4.1 General

Thorough literature review into type of manufacturing techniques used for optical coatings are reviewed to find the best way to coat optical films onto the scintillator materials. Factors considered are influence of the manufacturing technique on reflectivity of the coating, adhesiveness of the coating, influence on the materials refractive index, influence on the surface quality and composition of the deposited coating.

Thin film coatings have been synthesized by various deposition techniques such as thermal evaporation, sputtering, chemical vapour deposition, electro deposition, spray pyrolysis, solution growth technique, dip coating, chemical bath deposition, we will discuss and review some process to find advantages and disadvantages for use of optical coatings on scintillators. Article [14] discusses the influence of ion bombardment on optical properties during deposition technique. Relative humidity is a frequent problem when it comes to optical coating performance degradation after the coating has been deposited and the thin film is exposed to atmospheric conditions. Refractive index is highly influenced on the following process parameters; rate of deposition, pressure, vapour and substrate temperature with starting material and glow discharge being secondary influencing factors. On the other hand, adherence is highly influenced by the cleanliness of the substrate and the glow discharge although substrate material, evaporation method, rate, pressure, vapour and substrate temperature is also influencing factors.

4.1.1 Thermal and e-beam evaporation

Thermal evaporation requires a source of filament and metal sheet that contains the material to evaporate. An electric current heat a crucible. Knudsen cells are used to control evaporation rate and flow of vapour in form of a molecular regime. Recently ion beam plating has been introduced to the conventional thermal and e-beam evaporation technique. Ion plating involves a plasma discharge which guides the vapour flux onto the substrate. [26]

4.1.2 Cathodic arc evaporation

Research [27] shows that cathodic arc manufacturing technology can coat layers from range of 25 nm to 100 nm thickness with surface roughness of 2-4nm which means we get a smooth surface this result was obtained from pulsed cathodic arc plasma deposition technique, depositing copper doped, diamond like carbon coating. Cathodic arc technique is usually used to deposit hard/ dense coatings for tools to increase tool life and cutting performance. However optical coatings have also been coated with this technique due to adhesive, uniform and dense coating capabilities.

4.1.3 Sputtering PVD

An article [20] analysis the overall process stability by using a standard sputtering technique with cylindrical cathodes. Improved sputter yield distribution stability is achieved as the target is eroded homogeneously. It is noted that refractive index is generally decreased with higher deposition rate. In sputtering technique deposition rate is controllable and therefore desirable refractive index to a curtain degree is achievable.

PVD method is a manufacturing process to produce thin film coatings. Sputtering process is one of the most common types of PVD processes and involves plasma discharges which bombard the substrate by extracting material from target source. E.g. Under very high vacuum argon gas is feed into a vacuum chamber, which hits the target source material that has magnetic field behind it. A high voltage is applied to the target, to create plasma around the magnetic field, consisting of argon atoms, positively charged argon ions and free electrons. Positively charged argon ions are generated by electrons hitting the argon atoms as shown in Figure 5.1. Target is negatively charged and therefore the argon ions hit the target causing sputtering onto the substrate.

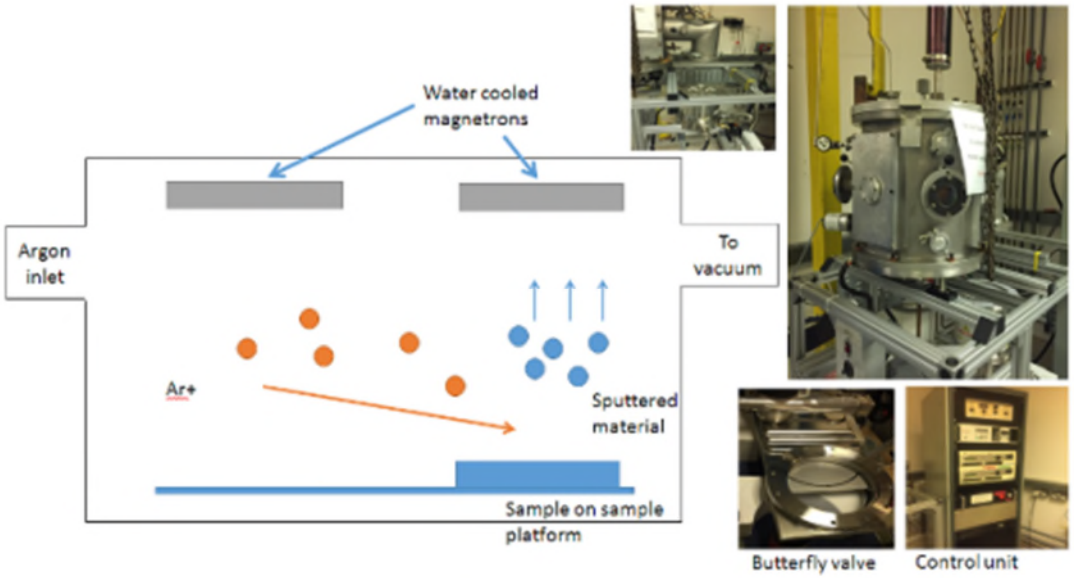

Figure 4-1: Process inside PVD chamber

This process is useful for many application types such as anti-corrosion, optical, wear resistant and aerospace industries because of the ability to produce very thin layer of coatings within nano meter scale with excellent mechanical properties. Design set-up of the chamber is illustrated in Figure 5.2.

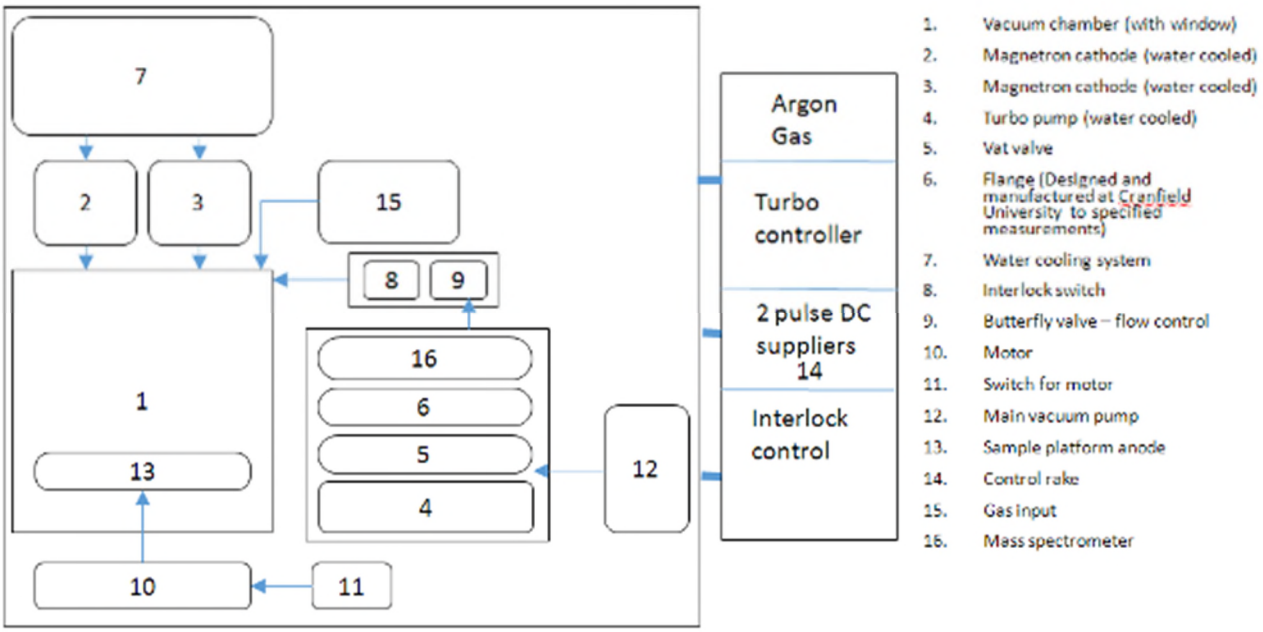

Figure 4-2: Physical vapor deposition chamber setup

4.1.4 Plasma Enhanced Chemical Vapor Deposition

Chemical vapour deposition is widely used within optical coatings for its several factors; produce dense coatings, good stoichiometry and uniformity over a large area however, there are material limitations due to high operating temperatures some materials may not be suitable for use. Plasma Enhanced CVD has shown to overcome this issue as cooler operating temperatures (e.g. 200 degrees C) with this process produce similar results. From article [6] we can find that refractive index and coating thickness can be controlled via PE-CVD with in situ measuring mechanism such as spectroscopic ellipsometry during deposition. Deposition rate of 1-18 nm/min where tested. Paper also showed that higher deposition rates resulted in higher refractive index on the coating.

4.1.5 Sol gel

An article [28] uses sol gel deposition technique to develop a highly reflective multi-layer coating. Alternating coatings of ZrO2 which has high refractive index was used together with SiO2 which has low refractive index. Experiment showed reflectivity of up to 99percent with a 20-layer coating with each layer being around 100nm thick.

4.2 Further enhancing the performance via manufacturing

To further improve light transportation from the time of photon emission within the scintillator due to matter interaction to the time of photon detection at the PMT, nano-indentation will be conducted on the proximal end of the scintillator. Through nano-indentation my aim is to achieve better light output gains as well as improved timing resolution. Further requirement for this type of material is to act as a light guide which allows a certain amount of light-sharing. Current technologies use a material in form of film tap or powder.

4.3 Conclusion

A high quality atomically arranged finish from PVD coating manufacturing process will give desirable surface finish to disallow any light loses and therefore be able to achieve high absorption percentages within ZnO fibres for fast response times. Moreover nano-indentation technique would greatly increase light output and timing resolution at the detector and scintillator interface. These manufacturing techniques will help to achieve results that of the simulation.

5 Methodology

5.1 General

This part of the research presents the design of my study, the research techniques and methods used throughout the research, how the subjects, instruments, software will yield the required data and how data is analysed. Methodology of my research is qualitative, there are set aims and objectives however the research design emerges as the study unfolds. A critical literature review on light transport in scintillators and manufacturing techniques is conducted. Literature review is analysed and concluded to guide towards the objectives.

5.2 Research

With the aim to design and optimise the heterostructure layout a comprehensive literature research is needed about current and previous scintillators together with physics of light transportation and interaction within scintillators. Therefore, initially a literature review on scintillators and response time of scintillation detectors. Scintillator materials (materials that exhibits scintillation when excited by ionizing radiation) are one of the main issues which influence the quality of the image, and dosage of radiation source used on patients for the studied medical imaging applications. Further study into latest most advanced scintillators such as LSO and LYSO which are used in currently used in PET scanners.

Furthermore, studying of the scintillation process, mechanisms and fundamental physics of matter interactions to understand why and how the scintillator properties influence the quality of the image. Timing resolution of scintillators are found to be one of the main issues in image quality as it significantly influences the noise variance in the reconstructed image.

Timing resolution in current scintillators is limited due to the intrinsic properties such as the Lutetium element inside the crystal. However, without this element the crystal will lose its other preferable properties such as stopping power and light output. A novel approach is taken to develop a heterostructure which is made of two scintillators in aim to improve timing resolution. Research into scintillators with very fast decay time has shown that ZnO is a very good candidate for the heterostructure design. LSO doped with Cerium is also chosen for its overall performance. An initial design is constructed via solid works. Using Geant4 I simulate the response time for gamma ray incidence on the 3D model.

Critical literature review on light guides and optical coatings for scintillators is studied. Further from literature review on light guides it is evident that light extraction is also a very important factor which needs to be considered. In response propose to develop a light extraction mechanism such as nano indentation for optimal light extraction.

Further research into nano-indentation is studied. Literature review on light transportation has also shown that manufacturing process is very important when performing optical coating on scintillators. A separate literature review onto manufacturing processes is studied to determine and select an appropriate process to perform optical coatings. Nano indentation has been commonly used and much research is taking place in this area for light extraction on scintillators.

5.3 Simulation via Geant4 tool-kit

5.3.1 Overview

Geant4 is a Monte Carlo computational tool-kit which operates via C++ language. I chose to use Geant4 simulation tool-kit as it has a well-established tool with several published reference papers in the Nuclear Instruments [29,30] and Methods in Physics Research [31] together with many journal publications, conference proceedings and reports. There is also a great community behind the tool-kit which are very helpful and supportive when approached. The tool-kit allows simulation of the passage of particles through matter and has wide scope of application use including but not limited to high energy, nuclear and accelerator physics and medical science which is our interest. For these qualities, well-established science related simulation tool-kit, is the main reason why Geant4 is selected for this research. In the following subsections, detailed steps of the simulation and program building is explained.

5.3.2 Examples

Geant4 has also an excellent user-friendly introduction to programming, tutorials and example programs relative to medical imaging. Use of OpNovice, Lxe and WLS examples have helped me greatly with building my own program as within the combination of these programs have relevant coding to realistically model the physics processes from charged particle, matter interaction and optics of scintillation. The simulation starts with a charged particle and ends with the detection of the ensuing optical photons on photo sensitive areas, all within the same event loop.

Optical photon production and other physics process within the three-example mentioned and Geant4 class packages have already developed and reviewed. My software program is built around these three examples(OpNovice, Lxe and WLS).

5.3.3 Program building

A program holds several classes including the main () class, where instructions can be given to call up relevant classes, but this does not usually hold direct information about a variable or execution. In the main () there are two tool-kit classes called run manager and UImanager and then all other classes that define the program. The runmanager class controls the flow of the program and manages the event loops within a run. To build and run a simulation a program needs to be constructed which has all the relevant classes to hold the necessary information. These are the several classes required to build the simulation: Detectorconstruction class: definition of materials and geometry of experiment Physicslist: particles and physics processes definition to be used in the simulation ActionInitialization: actions invoked during my simulation and to define the primary particle. Other user action classes: Additional classes required to run simulation (tracking of generated particles, defining initial state of the primary/secondary particles.)

5.3.4 Materials and Processes

Properties are expresses as a function of the photon's momentum. Material properties can be called from Geant4 material database or created with all the materials properties definitions. Research is conducted on the ZnO fibre coated and uncoated surfaces to determine if coating will influence the response time. Physical processes defined in the physics list will determine how the particles will interact with our materials. However, before we see any interaction we require a particle to be generated. This is done through a particle generator class where we generate a particle and define its momentum, direction of momentum, energy, time, position.

Number of photons generated is directly proportional to the energy lost during the step in the scintillation process. Once the optical photons are generated we ideally want to avoid any light loses by having a thin coating layer dictating the direction of travel of the optical photon. This is simulation of boundary effects, where the intersection between the medium and the surface layer is taken into consideration. This process is invoked via G4Navigator and G4 tracking volume.

Refractive index of the two media are stored in the G4MaterialPropertiesTable, reflection on a boundary implementation is also stored under this. Position and placement of the optical photon relative within the volume is defined via G4BoundaryProcess.

5.3.5 Program compiling

To compile all classes defined within the program, terminal command is used as follows:

1) source Geant4. / {call Geant4 source program

2) cd /OpticalPhotonTracking {path to directory folder

3) mkdir OpticalPhotonTracking_build {build a folder for compiling location

4) cd /OpticalPhotonTracking_build {changed directory to the build folder

5) cmake {compile files

6) make {make program, an executable target file OpticalPhotonTracking should be created from the outcome of this

7). /OpticalPhotonTracking {execute program

Visual program would open which allows us to run events on.

8) BeamOn 1

Sends a beam of gamma ray into the volume.

Once all the relevant classes are defined I compile the program into a build file which will determine if there are any errors. After successfully running my simulation program, a data file is generated which contained information of photon generations, movement through the medium for each photon and detection time.

5.3.6 Data analysis

Section 5.1.4 describes how we gather data from Geant4 simulation, to be able to analyse the data, python is used. Results of the data is displayed in graph form

to compare relevant data. The data from the graph justify the heterostructure performance for the response time. Absorption amount within different medium for the specific design is analysed. Different designs are compared with their absorption values within different mediums. Values for emission spectrum of the different materials used in the simulation is also analysed via python and data is compared with materials original emission spectrum to validate simulation results.

Geant4 tool-kit is used to simulate the fate of the created photons inside the scintillator considering optical properties and surfaces. Variables and parameters for the simulation is drawn from literature review and predefined optical transportation examples 55 within the Geant4 tool-kit Simulation data is assessed via python and represented in form of a graph in the report. For ultra-fast response time of photons created due to matter interactions to be detected as soon as possible. This means that the photon must take the shortest path towards the detector. To facilitate a fast transportation, a thin film coating between the scintillators interface is proposed to guide the generated photons towards the detector.

Number of photons detected, and their decay timing is outputted from the Geant4 simulation tool-kit onto a data file. The data file is extracted onto Microsoft Excel and displayed as a bar graph. Graph also displays grouped photons with a percentage chart on the right-hand side to illustrate number of fast and slowed photons and their quantities clearly.

Response timing for the first design, Design A shows that there is a great amount of event absorption and with only some absorption of ZnO we are already getting great response timing. An increase in the number of ZnO fibres within the composite volume we see a decrease in response timing as shown in figure 7.1. Design C is developed and tested in the program. In this design we increase the ZnO fibre sizes instead of number of fibres. We consequently have increased the volume of ZnO in the composite. Furthermore we have combined the design A, B and C with regards to each potential effect of each design to develop designs D and E.

5.4 Conclusion

Conducting appropriate research has helped to gather relevant information as well as good general knowledge of the topic throughout the degree. Geant4 has been a very powerful light transport simulation tool-kit which has helped with conducting simulation of gamma decay, generation of optical photons and their path of travel with respect to time, and ability to imitate real life conditions. Simulation illustrated in Figure 4.3 has been developed from the program code and illustrated from the visual console of the Geant4 program during and event run. Without Geant4 it would be a very expensive experiment to conduct with respect to time and money.

Methods used within this research has been chosen with respect to availability of resources, time management and required performance. Most of the research conducted was through development of the simulation program to conduct the experiment. However, literature review, data gathering and analysis, planning and organisation has also been major part of the research.

6 Results and Discussions

6.1 Simulation Results

Geant4 simulation results of gamma ray response on the heterostructure show expected coincidence response time by some calculations from absorption percentage during a 10000event run in Geant4 simulated randomly across the surface of the layout Table 7.1. The structure layout is yet to be optimised to achieve a faster response time. Figure 7.1 illustrates 5 different designs along the dotted line of coincidence response time, fastest response time achieved with design E where 10percent of 511keV was absorbed inside ZnO and the probability of absorption was the highest in ZnO at 22.5percent.

10,000 events of 511kev gamma ray energy onto each 3D model of heterostructure, as shown in Figure 7.1, we could fetch curtain data to calculate response time: the probability of event absorption, and the absorption percentage for individual materials (LSO and ZnO).

Initially gamma response for 5 different layouts is calculated, layout A can be used as an example:

Layout A has a probability of absorption of the 511keV energy which deposited in the ZnO is 3.3percent. Light output for ZnO is 18ph/kev and we use a quantum efficiency of 25 percent for the detector. So, to calculate the response time for layout A would be 115 picoseconds:

16.86keV x 18 = 303.53 photo electrons,

303.53 (photo electrons) x 0.25(quantum efficiency) = 75.88,

1/sq57.88 = 115ps

Layout	Event absorption %			Full absorption % of 511keV		Response time
	Full	Part	None	Full	Part	
A	32.7	18.9	48.4	96.7	3.3	115ps
B	25.0	22.1	52.9	6.5	93.5	82ps
C	25.4	21.7	52.9	7.1	92.9	78ps
D	26.2	22.5	51.3	9.7	90.3	67ps
E	23.6	22.5	53.9	10	90	66ps

Table 6-1: Gamma response time results

Starting with design A and using this as a foundation to work on we are able to discover onto which direction we want to move towards after we draw up the results of gamma event absorption. Layout A shows a great amount of absorption percentage of gamma, this is because most of the design volume is LSO. As ZnO fibre sizes are increase a decrease in gamma absorption is experienced. From event run of design A we can see that we are getting significant absorption percentage with relatively good response time, it is noted that there is a margin of flexibility in increasing the ZnO volume. A combination of large and small ZnO fibres in a LSO matrix desired event absorption is achieved as well as high absorption within ZnO. Gamma event absorption percentage is very important to reasons covered in earlier chapters and therefore we want to design a volume where both event absorption and ZnO absorption is maximised while keeping good overall event absorption.

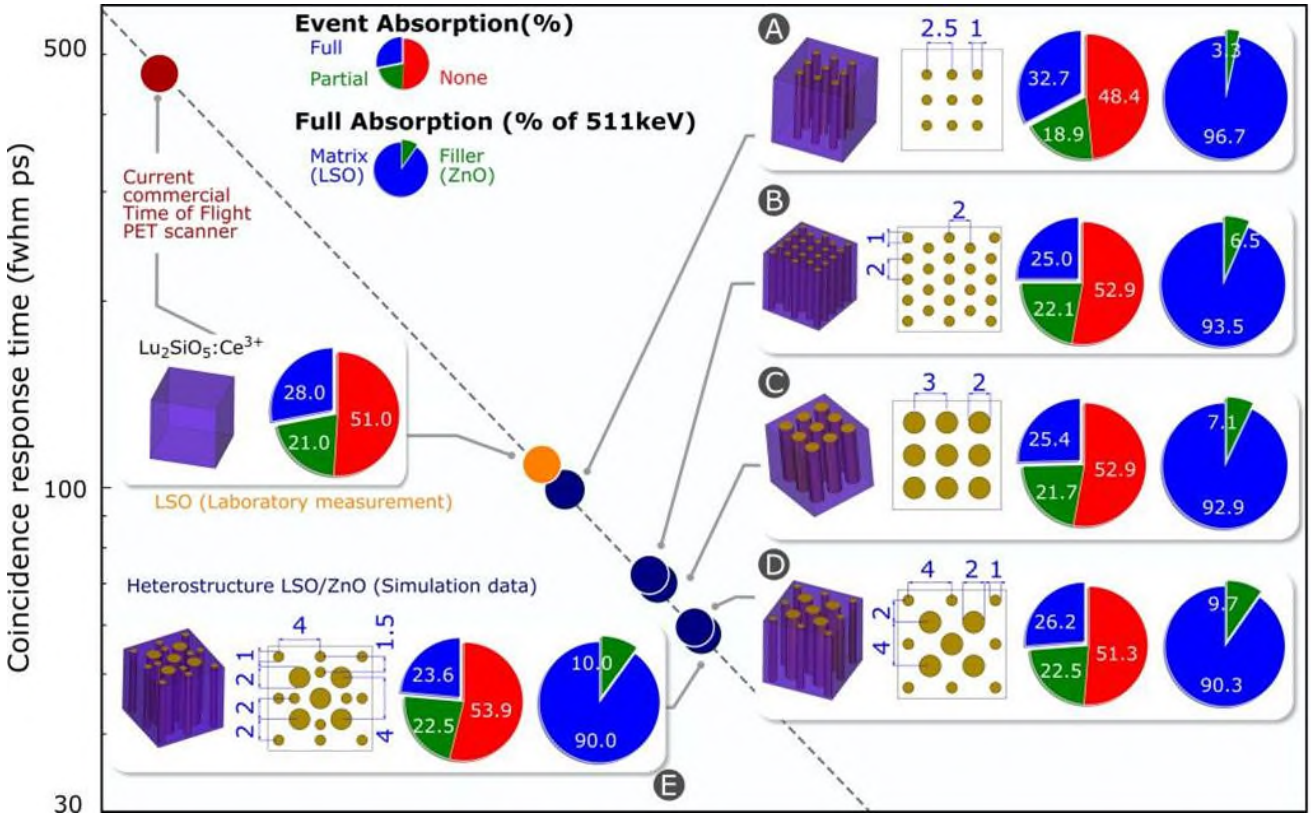

Figure 6-1: Gamma response time results

Full absorption probability is largely dependent on the LSO due to the material having high stopping power. Probability of absorption in ZnO is very important as it is directly proportional to the number of ultra-fast photons emitted by the structure. An optimal design however is still not developed, an optimal design would have a large proficiency to fully absorption of gamma ray and with maximum energy deposited in the ZnO.

Information processed can be saved into a text file. Depending on the verbose level we can control how much data to extract into the file. (e.g. Verbose 0 shows a low-profile information whereas verbose level 2 would give us a comprehensive analysis information however the text files size would be therefore much larger)

6.2 Simulation validation

Emission spectrum of LSO and ZnO showed peak emission of LSO to be at 3eV and ZnO at 3.28eV in Figure 7.2. Scintillation emission intensity for the LSO is much higher than in ZnO. Energy eV can also be looked in form of a wavelength, ZnO has a very sharp peak which shows that the time scale from excitation to de-excitation is very small compared to the LSO which occurs on a much longer time-scale.

Emission and absorption spectrum of the two materials, LSO and ZnO are observed and compared. Emission peak of LSO to be 420 nm wavelength and around 380 nm for ZnO. Other factors to account for is the transmittance of the 30 photons into the detector as it reaches at the surface of the PMT and the photon absorption coefficient. These are all dependant on the wavelength of the photon. Wavelength of maximum sensitivity of PMT is 400 nm. Emission wavelength of LSO and ZnO is 420 nm and 390 nm which are both close to maximum sensitivity are of the PMT.

Furthermore, the refractive index of the PMT is 1.5 and with ZnO at 1.73 and LSO at 1.82. To match the refractive index of the PMT a thin film with a refractive index of close to that of glass is required to create an optical coupling between the heterostructure and the PMT detector.

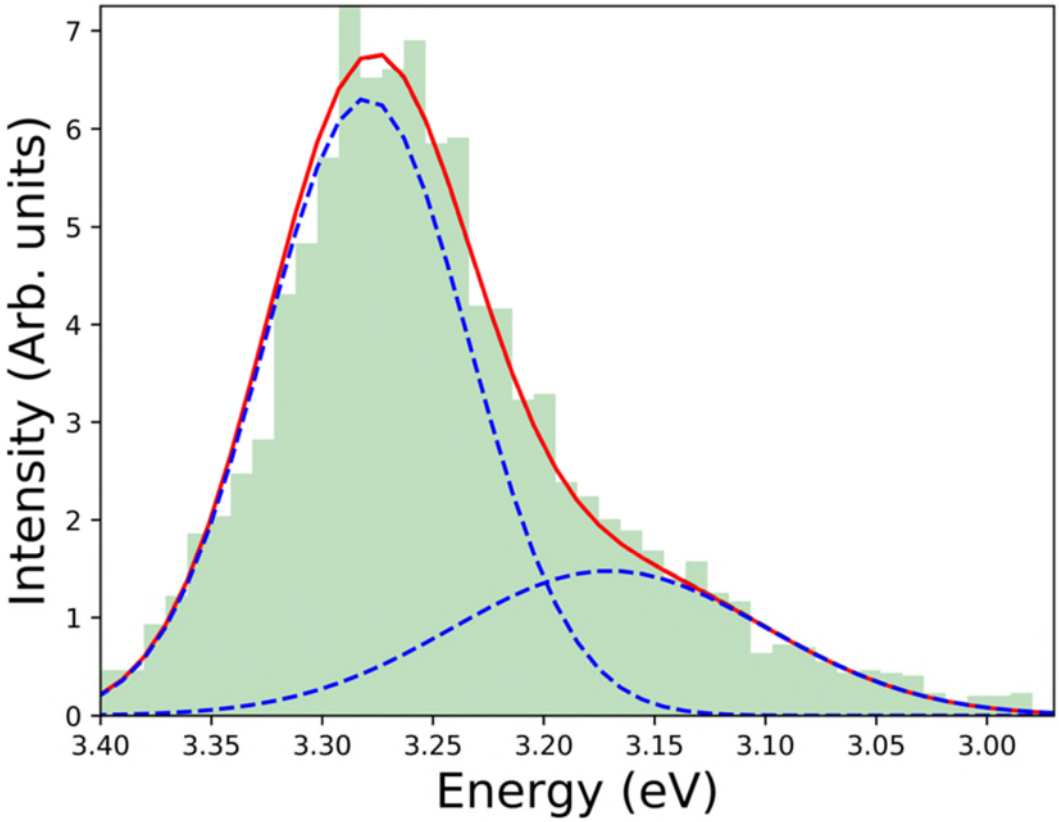

Figure 6-2: Emission Spectrum of ZnO

6.3 Analysis of optical photon detected

A gamma particle fired into the scintillator generates a secondary particle e- at -109 mm into the ZnO with kinetic energy of 279KeV following Compton scattering event. The e- particle deposits 268KeV of energy after a step length of 0.192mm and decay time of 0.153ps and which generates 147 optical photon particles. Initially we follow gamma particle as it enters the housing made of air it does not interact with and therefore no secondary particles are created. As the gamma particle enters the scintillator in step4 it a scintillation process happens as the gamma particle interacts via Compton scattering and an e- particle is created. In step5 the gamma particle interacts again this time via a photoelectric effect producing 2 e- secondary particles. 147 secondary scintillation photon particles are generated at the step6 following the Compton scattering process and 117 secondary scintillation photons are also created via photoelectric effect process.

Following each photon to its path we can see that the how many photons have successfully got to the PMT detector. 80 photons out of the total 254 where absorbed within the scintillator and 174 photons from the single gamma particle where able to reach the PMT. This was with the help of the reflective coating around the scintillator which helped guide these photons to the PMT.

6.4 Decay time from ZnO fibre

Average decay time of each photon at 1.39ns which is the total timing divided over 147 generated photons taken from the optical photon data shown in Figure7.5. A histogram of number of optical photons relative to decay time. Majority of the photons (64 of the 147) had decay time of 0.32ns-0.99ns, Figure7.3. Full data for a single event can be found in Event.data file in the appendix. From the data within the simulation program we can see optical photon on its individual step. We can see from Figure 7.4 the optical photons step where the optical photon invokes a transportation process from a step to another step a 0.191mm length between the two at the speed of light.

Figure7.3: Optical photon decay time histogram Several other details of the photon information are documented such as: the photons post and pre- step position relative to the x,y and z axis is also documented, the total energy at the different steps which tells us how much kinetic energy the photon has lost as it transported to the post step and the volume it is in such as scintillator outside the system or at the detector.

```
**PostStepDoIt (after all invocations):
   ++List of invoked processes
     1) Transportation
     2) eBrem (Forced)

   ++G4Step Information
     Address of G4Track    : 0xe5ff50
     Step Length (mm)      : 0.1918898121686891
     Energy Deposit (MeV)  : 0.2688526872886971
     ------------------------------------------------------------------------
       StepPoint Information              PreStep            PostStep
     ------------------------------------------------------------------------
        Position - x (mm)   :    -5.07983818709029  -5.111324442856827
        Position - y (mm)   :   -3.415325550594661  -3.401216308986355
        Position - z (mm)   :   -108.0244357318668  -108.0282295075353
        Global Time (ns)    :   0.3240791200912477  0.3242323962693603
        Local Time (ns)     :                      00.00015532761781125915
        Proper Time (ns)    :                      00.00010043444419076762
        Momentum Direct - x : -0.9070995180782566 -0.9070995180782566
        Momentum Direct - y :  0.4064785079001431  0.4064785079001431
        Momentum Direct - z : -0.1092963261846791 -0.1092963261846791
        Momentum - x (MeV/c): -0.5343798847773398                   -0
        Momentum - y (MeV/c):  0.2394598761074462                    0
        Momentum - z (MeV/c): -0.06438737649964957                  -0
        Total Energy (MeV)  :    0.779851597288697          0.51099891
        Kinetic Energy (MeV):   0.2688526872886971                    0
        Velocity (mm/ns)    :    226.4599566535394                    0
        Volume Name         :         scintillator       scintillator
        Safety (mm)         :                    0   3.287240244689401
        Polarization - x    :                    0                    0
        Polarization - y    :                    0                    0
        Polarization - Z    :                    0                    0
        Weight              :                    1                    1
        Step Status         :            Undefined     AlongStep Proc.
        Process defined Step:            Undefined               eIoni
     ------------------------------------------------------------------------

   ++List of secondaries generated (x,y,z,kE,t,PID):  No. of secodaries = 147
     [Note]Secondaries from AlongStepDoIt included.
     -5.089116168436647 -3.411168013368776 -108.0255536348701 3.198367058271885e-06 0.8518949275715012
opticalphoton
     -5.082406529401323 -3.414174655979948 -108.0247451911636 3.257580393579669e-06 0.8548639988504479
opticalphoton
     -5.095331745928368 -3.408382763664395 -108.0263025491529 3.28895575311442e-06 1.667586469523164
```

Figure 6-3: Optical photon data analysis

```
++List of secondaries generated (x,y,z,kE,t,PID):  No. of secodaries = 147
  [Note]Secondaries from AlongStepDoIt included.
  -5.089116168436647 -3.411168013368776 -108.0255536348701 3.198367058271885e-06 0.8518949275715012     opticalphoton
  -5.082406529401323 -3.414174655979948 -108.0247451911636 3.257580393579669e-06 0.8548639988504479     opticalphoton
  -5.095331745928368 -3.408382763664395 -108.0263025491529 3.28895575311442e-06 1.667586469523164     opticalphoton
  -5.080122124638686 -3.415198315921168 -108.0244699434724 3.3098992156560 89e-06 2.175611042497198     opticalphoton
  -5.097486782262491 -3.407417074744814 -108.0265622092557 3.233338585883236e-06 0.3254841097680116     opticalphoton
  -5.086724559392432 -3.412239712401 13 -108.0252654701462 3.227166851609803e-06 0.4867740534479292     opticalphoton
  -5.10716643200107 -3.403079546718045 -108.0277285092416 3.128558460298574e-06 2.089159374418048     opticalphoton
  -5.089568532857759 -3.410965305274178 -108.025608140212 3.284405499882059e-06 0.7366321564637722     opticalphoton
  -5.104479709498637 -3.404283488437961 -108.0274047863279 3.281271822576886e-06 1.231850911762325     opticalphoton
  -5.096190874055752 -3.407997781518164 -108.0264060654112 3.284152572149867e-06 0.5962493368291624     opticalphoton
  -5.092529390762995 -3.409638521300161 -108.0259648936717 3.29937023861971 9e-06 1.999982327876054     opticalphoton
  -5.089723205197631 -3.410895995368626 -108.025626776666 3.260521921153849e-06 2.654513385475962     opticalphoton
  -5.107555013975292 -3.402905420045137 -108.0277753294431 3.330692205309068e-06 0.5527374402115699     opticalphoton
  -5.098646603357733 -3.406897349688379 -108.0267019559783 3.176778890958854e-06 0.7150224939075622     opticalphoton
  -5.105219686099788 -3.403951899038207 -108.0274939460313 3.115574234055712e-06 1.592513897625735     opticalphoton
  -5.084068996189879 -3.413429691390971 -108.0249455016133 3.305956946917837e-06 0.3398915899920346     opticalphoton
  -5.085383039210492 -3.412840858263305 -108.0251038305196 3.184275836157911e-06 0.4138203503719542     opticalphoton
  -5.092013769378578 -3.409869575343077 -108.025902766505 3.235817735051424e-06 3.463239618212895     opticalphoton
  -5.098337102909641 -3.407036039300 52 -108.0266646643016 3.317429096499438e-06 2.606722473029 46     opticalphoton
  -5.102906732564653 -3.404988351911422 -108.0272152585014 3.249689207665351e-06 0.3488480456851211     opticalphoton
  -5.110346001804679 -3.401654756203027 -108.0281116152751 3.212075387948825e-06 0.8494467877498556     opticalphoton
  -5.083921232082427 -3.413495905662637 -108.0249276975314 3.294242561283337e-06 5.631652235787666     opticalphoton
  -5.107750852323889 -3.402817663323696 -108.0277989259853 3.286386507523224e-06 1.575379836040394     opticalphoton
  -5.084072661437887 -3.413428048964191 -108.0249459432386 3.265573320560007e-06 1.968028634076514     opticalphoton
  -5.091158332773 38 -3.410252903288859 -108.025799695037 7 3.237285759393806e-06 2.056710334838844     opticalphoton
  -5.084706004282495 -3.413144242998765 -108.0250222546518 3.31336627352533e-06 1.047826962597451     opticalphoton
  -5.090567347659199 -3.410517728418423 -108.0257284873031 3.095884807538601e-06 1.051501630480296     opticalphoton
  -5.104547671416757 -3.404253034161974 -108.0274129750533 3.113601691664719e-06 0.482669095233177     opticalphoton
```

Figure 6-4: Generated optical photons

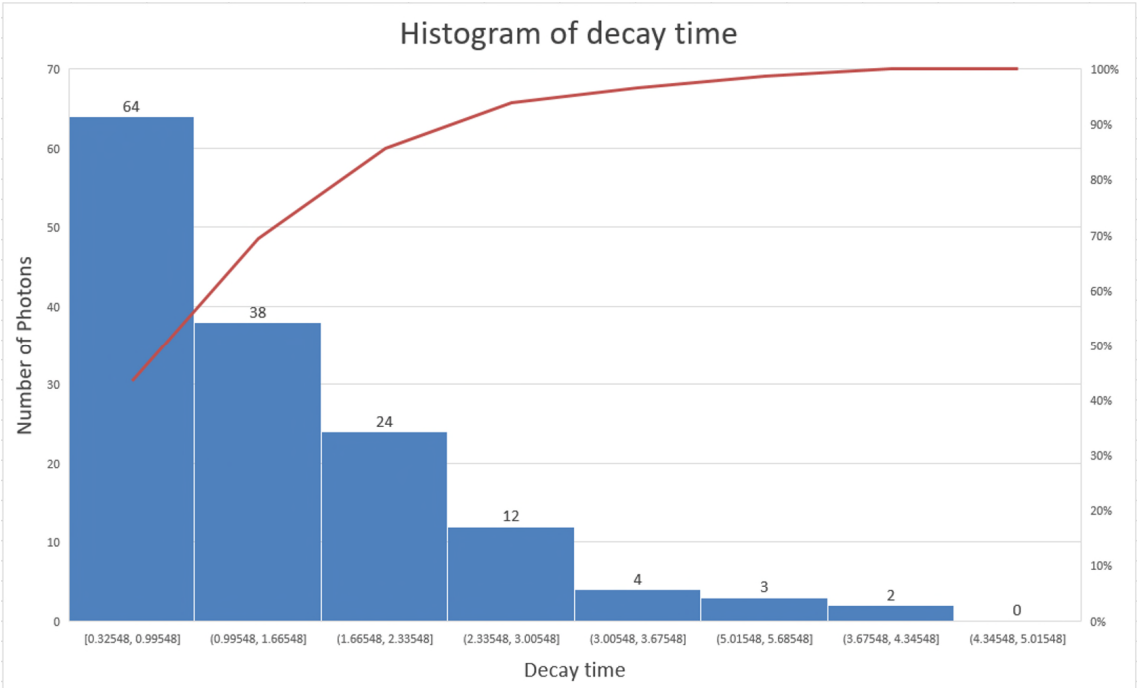

Figure 6-5: Optical photon decay time histogram

Most of the photons with low decay times as shown on the histogram shows a promising step forward for the search on ultra-fast decay timing. Considering that all these photons are coming only from the ZnO medium, there aren't many lower energy photons, meaning that the photon detection is maximised by the implemented surfaces. The reflective surfaces around the fibres are working well to direct the photons effectively to the detector and the surface layer between the detector and the ZnO fibre is effectively forming a good extracting photonic layer by refracting the photons effectively through to the detector.

7 Conclusion

Heterostructure layout use of ZnO and LSO scintillator materials is a novel approach technology for TOF-PET systems. It has several advantages which have been analysed and studied in this thesis. Heterostructure layout has shown a decreased decay timing, more than 40 times over the current scintillators used in the TOF-PET scanners. Simulation results have shown that with a good volumetric design of a heterostructure from LSO and ZnO, we are able to get desired properties, such as fast decay timing, high light output and high stopping power, to move the scintillation detection sensors to the next level.

Light output and energy resolution of the system has been maintained like the current technology with help of optimised design. Potential improvements to the system could be achieved with help of manufacturing techniques such as light extractions using nano-indentation.

8 Bibliography

[1] Florian Bauer. Detector Considerations for Time-of-Flight in Positron Emission tomography. PhD thesis, Department of Physics, Stockholm University, 2009.

[2] Eric Berg, Emilie Roncali, and Simon R Cherry. Optimizing light transport in scintillation crystals for time-of-flight pet: some experimental and optical monte carlo simulation study. Biomedical optics express, 6(6):2220–2230, 2015.

[3] Lisa Bläckberg, Mattias Klintenberg, Anders Ringbom, and Henrik Sjöstrand. Effects of surface coatings on the light collection in plastic scintillators used for radioxenon detection. Physica Scripta, 2012(T150):014007, 2012.

[4] Giacomo Borghi, Valerio Tabacchini, and Dennis R Schaart. Towards monolithic scintillator based tof-pet systems: practical methods for detector calibration and operation. Phys. Med. Biol., 61(13):4904–4928, 2016.

[5] Weerapong Chewpraditkul and Marek Moszynski. Scintillation properties of lu3al5o12, lu2sio5 and labr3 crystals activated with cerium. Physics Procedia, 22:218–226, 2011.

[6] M Chhowalla, KBK Teo, C Ducati, NL Rupesinghe, GAJ Amaratunga, AC Ferrari, D Roy, J Robertson, and WI Milne. Growth process conditions of vertically aligned carbon nanotubes using plasma enhanced chemical vapor deposition. Journal of Applied Physics, 90(10):5308–5317, 2001.

[7] F Daghighian, P Shenderov, KS Pentlow, MC Graham, B Eshaghian, CL Melcher, and JS Schweitzer. Evaluation of cerium doped lutetium oxyorthosilicate (lso) scintillation crystals for pet. IEEE transactions on nuclear science, 40(4):1045–1047, 1993.

[8] P Dorenbos, CWE Van Eijk, AJJ Bos, and CL Melcher. Afterglow and thermoluminescence properties of lu2sio5: Ce scintillation crystals. Journal of Physics: Condensed Matter, 6(22):4167, 1994.

[9] EI Gorokhova, GV Ananeva, VA Demidenko, and Rodnyĭ. Optical, luminescence, and scintillation properties of zno and zno: Ga ceramics.

[10] M Kapusta, P Szupryczynski, CL Melcher, M Moszynski, M Balcerzyk, AA Carey, W Czarnacki, MA Spurrier, and A Syntfeld. Non-proportionality and thermoluminescence of lso: Ce. In Nuclear Science Symposium Conference Record, 2004 IEEE, volume 2, pages 822–828. IEEE, 2004.

[11] Arno Knapitsch, Etiennette Auffray, CW Fabjan, Jean-Louis Leclercq, Paul Lecoq, Xavier Letartre, and Christian Seassal. Photonic crystals: A novel approach to enhance the light output of scintillation based detectors. Nuclear Instruments and Methods in Physics Research Section A: Accelerators, Spectrometers, Detectors and Associated Equipment, 628(1):385–388, 2011.

[12] P Lecoq, E Auffray, S Brunner, H Hillemanns, P Jarron, A Knapitsch, T Meyer, and F Powolny. Factors influencing time resolution of scintillators and ways to improve them. IEEE Transactions on Nuclear Science, 57(5):2411–2416, 2010.

[13] Francis Loignon-Houle, Mélanie Bergeron, Catherine M Pepin, Serge A Charlebois, and Roger Lecomte. Simulation of scintillation light output in lyso scintillators through a full factorial design. Physics in medicine and biology, 62(2):669, 2017.

[14] PJ Martin. Ion-based methods for optical thin film deposition. Journal of materials science, 21(1):1–25, 1986.

[15] Jitka Mohelnikova. Materials for reflective coatings of window glass applications. Construction and Building materials, 23(5):1993–1998, 2009.

[16] MA Mosleh-Shirazi, W Swindell, and PM Evans. Optimization of the scintillation detector in a combined 3d megavoltage ct scanner and portal imager. Medical physics, 25(10):1880–1890, 1998.

[17] John S Neal, John T Mihalczo, David Koltick, and Charles Cooper. Update on a zno: Ga alpha particle detector for a portable neutron generator for the nuclear materials identification system (nmis). 2006.

[18] SD Noble, A Boeré, T Kondratowicz, TG Crowe, RB Brown, and DA Naylor. Characterization of a low-cost diffuse reflectance coating. Canadian Journal of Remote Sensing, 34(2):68–76, 2008.

[19] A Polychronopoulou, D Thanasas, N Giokaris, A Karabarbounis, D Maintas, CN Papanicolas, and E Stiliaris. Study of the optical properties of continuous and pixelated scintillation crystals. Journal of Instrumentation, 4(09): P09002, 2009.

[20] D Rademacher, S Kreher, M Rudin, M Vergöhl, and T Zickenrott. Manufacturing of high-precision optical coatings using a novel sputtering system. In Society 45of Vacuum Coaters55th Annual Technical Conference, Santa Clara, California, USA, volume 28, 2012.

[21] PA Rodnyi and IV Khodyuk. Optical and luminescence properties of zinc oxide. Optics and Spectroscopy, 111(5):776–785, 2011.

[22] Emilie Roncali, Mariele Stockhoff, and Simon R Cherry. An integrated model of scintillator-reflector properties for advanced simulations of optical transport. Phys. Med. Biol., 2017.

[23] P Schauer and R Autrata. Light transport in single-crystal scintillation detectors in sem. Scanning, 14(6):325–333, 1992.

[24] Horst Schölermann and Horst Klein. Optimizing the energy resolution of scintillation counters at high energies. Nuclear Instruments and Methods, 169(1):25–31, 1980.

[25] Virginia Ch Spanoudaki and Craig S Levin. Photo-detectors for time of flight positron emission tomography (tof-pet). Sensors, 10(11):10484–10505, 2010.

[26] A Tanuševski and Dirk Poelman. Optical and photoconductive properties of sns thin films prepared by electron beam evaporation. Solar energy materials and solar cells, 80(3):297–303, 2003.

[27] J Vyskočil and J Musil. Cathodic arc evaporation in thin film technology. Journal of Vacuum Science & Technology A: Vacuum, Surfaces, and Films, 10(4):1740–1748, 1992.

[28] Qinyuan Zhang, Jun Shen, Jue Wang, Guangming Wu, and Lingyan Chen. Sol–gel derived zro 2–sio 2 highly reflective coatings. International Journal of Inorganic Materials, 2(4):319–323, 2000.

[29] Sartini, L., Simeone, F., Pani, P., Lo Bue, N., Marinaro, G., Grubich, A., Lobko, A., Etiope, G., Capone, A., Favali, P. and Gasparoni, F., 2010. Nuclear instruments and methods in physics research section a: Accelerators, spectrometers, detectors and associated equipment. *Nuclear Instruments and Methods in Physics Research A.*

[30] Allison, J., Amako, K., Apostolakis, J., Araujo, H.A.A.H., Dubois, P.A., Asai, M.A.A.M., Barrand, G.A.B.G., Capra, R.A.C.R., Chauvie, S.A.C.S., Chytracek, R.A.C.R. and Cirrone, G.A.P., 2006. Geant4 developments and applications. *IEEE Transactions on nuclear science*, *53*(1), pp.270-278.

[31] Agostinelli, S., Allison, J., Amako, K.A., Apostolakis, J., Araujo, H., Arce, P., Asai, M., Axen, D., Banerjee, S., Barrand, G.2. and Behner, F., 2003. GEANT4—a simulation tool-kit. *Nuclear instruments and methods in physics research section A: Accelerators, Spectrometers, Detectors and Associated Equipment*, *506*(3), pp.250-303.

[32] Figure 3.1, Illustration of Types of Ionizing Radiation, By Jens Maus URL: http://jens-maus.de/ [Public domain], via Wikimedia Commons

[33] Figure 3.3, Illustration of Types of Ionizing Radiation, URL: https://www.mirion.com/introduction-to-radiation-safety/types-of-ionizing-radiation/

[34] Figure 3.4, Illustration of Interaction with matter, URL: http://www.sprawls.org/resources/INTERACT/ mindmap.htm

[35] Figure 3.5, Illustration of Compton effect, Chapter 27, Early Quantum Theory and Models of the Atom, URL: https://slideplayer.com/slide/3835790/13/images/22/

[36] Figure 3.6, Illustration of photoelectric effect, The Spectrum, URL: http://www.physics.utah.edu/spectrum/index.php/demolicious-physics/76-simple-photoelectric-effect

[37] Figure 3.7, Illustration of Bremsstrahlung production, Slide 23/77, X-Ray Technology, URL: https://slideplayer.com/slide/6188331/

[38] Figure 4.2, Illustration of the periodic table of elements, URL: https://ptable.com/Images/periodic_table.png

9 Appendix A

Emission spectrum
Figure A.1: Emission spectrum of LSO
Figure A.2: emission spectrum of ZnO

10 Appendix B

Gantt Chart

11 Appendix C

Simulation Data
see electronic attachment as the data file is too large for printing